

Published in final edited form as:

Vib Spectrosc. 2005 July 29; 38(1-2): 107–114.

Infrared spectroscopic characterization of mineralized tissues

Adele L. Boskey^{a,*} and Richard Mendelsohn^b

^a Musculoskeletal Integrity Program, Research Division, Hospital for Special Surgery, 535 E. 70th St., New York, NY 10021, USA

^b Department of Chemistry, Rutgers University, Newark, NJ, USA

Abstract

Vibrational spectroscopy (Infrared and Raman), and in particular micro-spectroscopy and micro-spectroscopic imaging has been used to characterize developmental changes in bone and other mineralized tissues, to monitor these changes in cell cultures, and to detect disease and drug-induced modifications. Examples of the use of infrared micro-spectroscopy and micro-spectroscopic imaging are discussed in this review.

Keywords

Vibrational spectroscopy; Cell culture; Infrared and Raman

1. Introduction

The mineralized tissues found in vertebrates can be subdivided into those, which develop through normal physiologic processes (e.g., bones, teeth, calcified cartilage, etc.), and those that form through pathologic processes (e.g., atherosclerotic plaques, kidney and salivary stones, and other pathologic deposits). Table 1 lists examples of these two types of calcified tissues, and the mineral phase or phases they most frequently contain. As can be seen from the table, all the physiologic deposits contain an analogue of the naturally occurring mineral, hydroxyapatite ($\text{Ca}_{10}(\text{PO}_4)_6(\text{OH})_2$ (HA). With the exception of the enamel of teeth, all the other physiologically mineralized tissues are deposited upon a collagen matrix, while that of enamel is collagen-free. Because the spectra of these mineral components are quite distinct, vibrational spectroscopy (Raman and infrared) has been extensively used to study all of these tissues providing information on the nature of the mineral phases present, quantitative information on the changes in mineral and matrix composition as mineralization occurs, and the nature and amounts of substituents in the mineral (e.g., [1-7]). In accord with the theme of this issue, this review is focused on IR microscopy and microscopic imaging for characterization and diagnoses of normal and diseased mineralized tissues. Specifically, we shall examine developmental studies of bones and teeth using whole tissues and cell cultures, pathologic calcifications, and the study of bone disease.

In addition to the hyperspectral images (x - y position, z intensity or value of parameter in question) showing the distribution of the phosphate ν_1 , ν_3 , ν_2 carbonate or amide I peaks (Fig. 1), several calculated parameters have been validated for the HA-containing tissues. The ratio of the area of the ν_1 , ν_3 phosphate vibration (900 – 1200 cm^{-1}) to that of the amide I vibration is directly related to the chemically determined mineral content (ash weight) [8,9]. Carbonate to amide I ratios or carbonate to phosphate ratios indicate the extent of carbonate incorporation in the hydroxyapatite lattice, and curve-fitting of the carbonate band reveals whether the

*Corresponding author. Tel.: +1 212 606 1453; fax: +1 212 472 5331. E-mail address: boskeya@hss.edu (A.L. Boskey).

carbonate has replaced hydroxide (A-type) or phosphate (B-type) in the apatite lattice [10]. The relative areas of sub-bands at 1060 cm^{-1} [11] or the ratio of the 1030 and 1020 cm^{-1} sub-bands [12] correlate linearly with the HA crystal size and perfection in the *c*-axis direction as determined by X-ray diffraction analyses. In IR imaging, this ratio is often expressed as a ratio of peak height intensities [13] because it is time consuming to curve fit the number of spectra in a single image, not to mention multiple images. The areas of sub-bands at 1660 and 1686 cm^{-1} (or their intensity ratios) is related to the amount of non-reducible as contrasted with reducible collagen-cross links [14,15]. Hyperspectral images enable visualization of each of these parameters in the systems under examination.

2. Characterization of the development of physiologically mineralized tissues

The formation of the mineralized tissues starts with the patterning of the skeletal elements [16] and proceeds through the differentiating and proliferation of the cells that synthesize the matrices upon which the mineral is deposited. Vibrational micro-spectroscopy has been used to describe the progression of mineralization in the developing tooth [17], the conversion of calcified cartilage into bone within the epiphyseal growth plate [18-20], tendon calcification [21,22] and bone maturation [23-28]. Examining mice in which protein expression was ablated by gene-deletion (knockout) or enhanced by over-expression (transgenics) by vibrational micro-spectroscopy and imaging has allowed the impact of specific matrix proteins and cytokines to be evaluated. For example, deletion of transforming growth factor beta-1 was shown to result in a significant reduction in mineral content, mineral crystallinity and collagen cross-links in the secondary ossification center and cortical bones, consistent with a mechanism of impaired bone maturation in the TGF-beta-1 null mice [29]. Similarly, over-expression of the receptor for insulin growth factor 1 was shown to alter the pattern of mineralization [30].

The ablation or over-expression of genes for specific bone, cartilage and tooth specific matrix proteins in mice (Table 2, [31-39]) often produce mild changes in tissue phenotype which may not be readily detectable by standard radiological or histochemical techniques. Distinct effects on mineral content and mineral crystal size and perfection and collagen cross-link distributions can be determined by vibrational spectroscopic imaging. The changes noted in the majority of cases validate predictions made from solutionbased studies.

3. Characterizing the mineral in cell culture

Physiologic mineral deposition is regulated by cells. The cells produce the extracellular matrix (predominately collagen) that supports the deposition of the mineral and the non-collagenous matrix proteins that regulate the site and habit of the mineral crystals [40]. The cells also regulate the flux of ions and the synthesis of macromolecules that facilitate initial mineral deposition. While IR analyses of homogenized cultures can provide information on the characteristics of the mineral that is present in a homogenized culture (e.g., [41-47]), IR microscopy and imaging provides additional information by allowing visualization of the distribution of mineral and matrix at discrete sites within the culture [48-56]. This enables investigators to ask specific questions about temporal and spatial variations within mineralizing cultures and about the environments of specific cell types. The effects of genetic or chemical modulation of the cells and matrix in the culture systems can be monitored as the culture develops, and sites close to and distant from the modified cells.

To date while IR has been applied to bone forming cells (osteoblast cultures) [40-48], dentin forming odontoblasts [49-51] and calcifying cartilage cells (chondrocyte cultures) [52-56]. IR imaging has only been applied in a limited number of cases, in one to distinguish the different ways in which osteoblasts behave on different prepared surfaces that might eventually be used for tissue engineering [48], and in others to define the progression of calcification in differentiating mesenchymal cell cultures treated with the cytokine BMP-6 [56]. Fig. 2 shows

some typical images of the mineral content, crystallinity and collagen cross-link ratio in mineralizing osteoblast and chondrocyte cultures. These images show that the mineral is deposited upon a collagen matrix, there is a gradient of mineral deposition and a gradient of crystal sizes. The advantage of such cultures is that temporal changes can be characterized without having to manipulate animals; the disadvantage is that these cultures do not completely mimic what happens in the body where there are a multitude of cells and metabolic processes that may have direct and indirect effects on mineralization.

4. Characterizing the mineral and matrix in pathologic calcifications

While IR or Raman examination of homogenized deposits is routinely used to identify the nature of the mineral deposit present [58-64], it often happens that there is more than one phase, and investigators are interested in which came first or in what the nature of the interaction is between the matrix and the deposit. We have recently applied IR imaging to the study of juvenile dermatomyositis, a disease in children in which calcific deposits form in muscle and fat. These deposits are generally surgically removed for relief of symptoms, and working with Dr. Lauren Pachman (Northwestern University), we not only demonstrated the presence of hydroxyapatite in these deposits, but we also noted the association of the mineral and lipid (Fig. 3). This feature would be missed in standard KBr pellets, where the matrix is often defatted before pellet preparation. The figure illustrates the type of information that can be learned from such diagnostic surveys. The vibrational spectroscopic image of a calcific deposit provides more information than routine histology, where separate stains must be used, and phase identification is often based on polarization studies of unstained sections. Where multiple phases are present, imaging may be the most rapid way of identifying which phases are in the center and periphery of deposits, rather than needing to dissect layers of the deposit for such analysis.

5. Characterizing the mineral and matrix in bone diseases

A recent concern in the bone community is the “quality of the bone” because it is believed to be most predictive of when a bone will fracture in patients with osteoporosis. According to a recent NIH consensus conference, “Osteoporosis is defined as a skeletal disorder characterized by compromised bone strength predisposing to an increased risk of fracture. Bone strength reflects the integration of two main features: bone density and bone quality” [65]. The mechanical competence of bone and hence its risk of fracture are dependent on the bones' mass, architecture and material quality [66-69]. The IR parameters that may be related to bone quality are mineral content, mineral crystallinity and collagen cross-link ratio. IR images of normal bones show a broad distribution of these parameters while the distribution in osteoporotic bones is narrow, and mineral content tends to be decreased while the other parameters are increased (Fig. 4). IR imaging of bone biopsies thus becomes useful for diagnosing the quality of bone, above and beyond what can be learned from routine histologic studies [70-72].

Changes in bone quality in other diseases such as osteogenesis imperfecta [73-75], osteopetrosis [76], osteomalacia [77] and bone tumors [78] both prior to and after treatment may also be evaluated using these techniques. For example, the effects of alendronate treatment of a mouse model of osteogenesis imperfecta [79], parathyroid treatment of a monkey model of osteoporosis [80], and risedronate therapy in a rodent model of osteoporosis [81] have shown the alterations in mineral and matrix quality caused by these therapies. Similarly, there are a few studies of the effects of therapeutics currently in use for the treatment and prevention of osteoporosis in human biopsies [82-85].

Each of these studies demonstrates changes in the spatial distribution of mineral and matrix properties in the biopsied tissues. These changes in the future may not only be used for

diagnostic purposes, but also to select the most effective therapy for treatment of different bone diseases.

Uncited reference

[57].

Acknowledgments

Studies in the manuscript were supported by NIH grants AR041325, AR037661 and DE04141.

References

1. Grant GA, Wener MH, Yaziji H, Futran N, Bronner MP, Mandel N, Mayberg MR. Destructive tophaceous calcium hydroxyapatite tumor of the infratemporal fossa. Case report and review of the literature. *J Neurosurg* 1999;90(1):148–152. [PubMed: 10413170]
2. Derfus BA, Rachow JW, Mandel NS, Boskey AL, Buday M, Kushnaryov VM, Ryan LM. Articular cartilage vesicles generate calcium pyrophosphate dihydrate-like crystals in vitro. *Arthritis Rheum* 1992;35(2):231–240. [PubMed: 1734912]
3. Feinberg J, Boachie-Adjei O, Bullough PG, Boskey AL. The distribution of calcific deposits in intervertebral discs of the lumbosacral spine. *Clin. Orthop* 1990;(254):303–310. [PubMed: 2157573]
4. Arlet J, Legros R, Savio JL, Bonel G. Crystallographic identification of a calcium deposit in calcified pericarditis associated with articular chondrocalcinosis. *Bone* 1986;7(3):187–191. [PubMed: 3768196]
5. Li C, Ebenstein D, Xu C, Chapman J, Saloner D, Rapp J, Pruitt L. Biochemical characterization of atherosclerotic plaque constituents using FTIR spectroscopy and histology. *J. Biomed. Mater. Res* 2003;64A(2):197–206.
6. Silveira L Jr, Sathiaiah S, Zangaro RA, Pacheco MT, Chavantes MC, Pasqualucci CA. Correlation between near-infrared Raman spectroscopy and the histopathological analysis of atherosclerosis in human coronary arteries. *Lasers Surg. Med* 2002;30:290–297. [PubMed: 11948599]
7. Hamada J, Ono W, Tamai K, Saotome K, Hoshino T. Analysis of calcium deposits in calcific periarthritis. *J. Rheumatol* 2001;28(4):809–813. [PubMed: 11327256]
8. Pienkowski D, Doers TM, Monier-Faugere MC, Geng Z, Camacho NP, Boskey AL, Malluche HH. Calcitonin alters bone quality in beagle dogs. *J. Bone Miner. Res* 1997;12(11):1936–1943. [PubMed: 9383698]
9. Faibish D, Boivin G, Boskey AL. Bone. in press
10. Mayer I, Schneider S, Sydney-Zax M, Deutsch D. Thermal decomposition of developing enamel. *Calcif. Tissue Int* 1990;46(4):254–257. [PubMed: 2108795]
11. Pleshko N, Boskey A, Mendelsohn R. Novel infrared spectroscopic method for the determination of crystallinity of hydroxyapatite minerals. *Biophys. J* 1991;60(4):786–793. [PubMed: 1660314]
12. Paschalis EP, Betts F, Mendelsohn R, Boskey AL. Fourier transform infrared spectroscopy of the solution-mediated conversion of amorphous calcium phosphate to hydroxyapatite: new correlations between X-ray diffraction and infrared data. *Calcif. Tissue Int* 1996;58(1):9–16. [PubMed: 8825233]
13. Boskey AL, Moore DJ, Amling M, Canalis E, Delany AM. Infrared analysis of the mineral and matrix in bones of osteonectin-null mice and their wildtype controls. *J. Bone Miner. Res* 2003;18(6):1005–1011. [PubMed: 12817752]
14. Paschalis EP, Verdelis K, Doty SB, Boskey AL, Mendelsohn R, Yamauchi M. Spectroscopic characterization of collagen cross-links in bone. *J. Bone Miner. Res* 2001;16(10):1821–1828. [PubMed: 11585346]
15. Paschalis EP, Recker R, DiCarlo E, Doty SB, Atti E, Boskey AL. Distribution of collagen cross-links in normal human trabecular bone. *J. Bone Miner. Res* 2003;18(11):1942–1946. [PubMed: 14606505]
16. Mariani FV, Martin GR. Deciphering skeletal patterning: clues from the limb. *Nature* 2003;423(6937):319–325. [PubMed: 12748649]
17. Verdelis K, Crenshaw MA, Paschalis EP, Doty S, Atti E, Boskey AL. Spectroscopic imaging of mineral maturation in bovine dentin. *J. Dent. Res* 2003;82(9):697–702. [PubMed: 12939353]

18. Mendelsohn R, Hassankhani A, DiCarlo E, Boskey A. FT-IR microscopy of endochondral ossification at 20 μ m spatial resolution. *Calcif. Tissue Int* 1989;44(1):20–24. [PubMed: 2492884]Erratum in: *Calcif. Tissue Int.* 45 (July 1989) (1) 62
19. Rey C, Beshah K, Griffin R, Glimcher MJ. Structural studies of the mineral phase of calcifying cartilage. *J. Bone Miner. Res* 1991;6(5):515–525. [PubMed: 2068959]
20. Boskey AL, Maresca M, Wikstrom B, Hjerpe A. Hydroxyapatite formation in the presence of proteoglycans of reduced sulfate content: studies in the brachymorphic mouse. *Calcif. Tissue Int* 1991;49(6):389–393. [PubMed: 1818763]
21. Gadaleta SJ, Camacho NP, Mendelsohn R, Boskey AL. Fourier transform infrared microscopy of calcified turkey leg tendon. *Calcif. Tissue Int* 1996;58(1):17–23. [PubMed: 8825234]
22. Gadaleta SJ, Landis WJ, Boskey AL, Mendelsohn R. Polarized FT-IR microscopy of calcified turkey leg tendon. *Connect. Tissue Res* 1996;34(3):203–211. [PubMed: 9023049]
23. Paschalis EP, DiCarlo E, Betts F, Sherman P, Mendelsohn R, Boskey AL. FTIR microspectroscopic analysis of human osteonal bone. *Calcif. Tissue Int* 1996;59(6):480–487. [PubMed: 8939775]
24. Ou-Yang H, Paschalis EP, Mayo WE, Boskey AL, Mendelsohn R. Infrared microscopic imaging of bone: spatial distribution of $\text{CO}_3^{(2-)}$. *J. Bone Miner. Res* 2001;16(5):893–900. [PubMed: 11341334]
25. Miller LM, Novatt JT, Hamerman D, Carlson CS. Alterations in mineral composition observed in osteoarthritic joints of cynomolgus monkeys. *Bone* 2004;35(2):498–506. [PubMed: 15268902]
26. Boskey AL. Bone mineral crystal size. *Osteoporos. Int* 2003;14(Suppl 5):16–21. [PubMed: 14504701]
27. Paschalis EP, Recker R, DiCarlo E, Doty SB, Atti E, Boskey AL. Distribution of collagen cross-links in normal human trabecular bone. *J. Bone Miner. Res* 2003;18(11):1942–1946. [PubMed: 14606505]
28. Tarnowski CP, Ignelzi MA Jr, Morris MD. Mineralization of developing mouse calvaria as revealed by Raman microspectroscopy. *J. Bone Miner. Res* 2002;17(6):1118–1126. [PubMed: 12054168]
29. Atti E, Gomez S, Wahl SM, Mendelsohn R, Paschalis E, Boskey AL. Effects of transforming growth factor-beta deficiency on bone development: a Fourier transform-infrared imaging analysis. *Bone* 2002;31(6):675–684. [PubMed: 12531561]
30. Paschalis EP, Jacenko O, Olsen B, Mendelsohn R, Boskey AL. Fourier transform infrared microspectroscopic analysis identifies alterations in mineral properties in bones from mice transgenic for type X collagen. *Bone* 1996;19(2):151–156. [PubMed: 8853859]
31. Camacho NP, Landis WJ, Boskey AL. Mineral changes in a mouse model of osteogenesis imperfecta detected by Fourier transform infrared microscopy. *Connect. Tissue Res* 1996;35(1–4):259–265. [PubMed: 9084664]
32. Paschalis EP, Jacenko O, Olsen B, deCrombrughe B, Boskey AL. The role of type X collagen in endochondral ossification as deduced by Fourier transform infrared microscopy analysis. *Connect. Tissue Res* 1996;35(1–4):371–377. [PubMed: 9084677]
33. Xu T, Bianco P, Fisher LW, Longenecker G, Smith E, Goldstein S, Bonadio J, Boskey A, Heegaard AM, Sommer B, Satomura K, Dominguez P, Zhao C, Kulkarni AB, Robey PG, Young MF. Targeted disruption of the biglycan gene leads to an osteoporosis-like phenotype in mice. *Nat. Genet* 1998;20(1):78–82. [PubMed: 9731537]
34. Boskey AL, Gadaleta S, Gundberg C, Doty SB, Ducy P, Karsenty G. Fourier transform infrared microspectroscopic analysis of bones of osteocalcin-deficient mice provides insight into the function of osteocalcin. *Bone* 1998;23(3):187–196. [PubMed: 9737340]
35. Boskey AL, Spevak L, Paschalis E, Doty SB, McKee MD. Osteopontin deficiency increases mineral content and mineral crystallinity in mouse bone. *Calcif. Tissue Int* 2002;71(2):145–154. [PubMed: 12073157]
36. Boskey AL, Moore DJ, Amling M, Canalis E, Delany AM. Infrared analysis of the mineral and matrix in bones of osteonectinnull mice and their wildtype controls. *J. Bone Miner. Res* 2003;18(6):1005–1011. [PubMed: 12817752]
37. Misof BM, Roschger P, Tesch W, Baldock PA, Valenta A, Messmer P, Eisman JA, Boskey AL, Gardiner EM, Fratzl P, Klaushofer K. Targeted overexpression of Vitamin D receptor in osteoblasts increases calcium concentration without affecting structural properties of bone mineral crystals. *Calcif. Tissue Int* 2003;73(3):251–257. [PubMed: 14667138]

38. Kozloff KM, Carden A, Bergwitz C, Forlino A, Uveges TE, Morris MD, Marini JC, Goldstein SA. Brittle IV mouse model for osteogenesis imperfecta IV demonstrates postpubertal adaptations to improve whole bone strength. *J. Bone Miner. Res* 2004;19(4):614–622. [PubMed: 15005849]
39. Anderson HC, Sipe JB, Hessle L, Dhanyamraju R, Atti E, Camacho NP, Millan JL, Dhanyamraju R. Impaired calcification around matrix vesicles of growth plate and bone in alkaline phosphatase-deficient mice. *Am. J. Pathol* 2004;164(3):841–847. [PubMed: 14982838]Erratum in: *Am. J. Pathol.* 164 (May 2004) (5), 873
40. Rey C, Kim HM, Gerstenfeld L, Glimcher MJ. Characterization of the apatite crystals of bone and their maturation in osteoblast cell culture: comparison with native bone crystals. *Connect. Tissue Res* 1996;35(1–4):343–349. [PubMed: 9084674]
41. Motta A, Migliaresi C, Faccioni F, Torricelli P, Fini M, Giardino R. Fibroin hydrogels for biomedical applications: preparation, characterization and in vitro cell culture studies. *J. Biomater. Sci. Polym. Ed* 2004;15(7):851–864. [PubMed: 15318796]
42. Luppen CA, Smith E, Spevak L, Boskey AL, Frenkel B. Bone morphogenetic protein-2 restores mineralization in glucocorticoid-inhibited MC3T3-E1 osteoblast cultures. *J. Bone Miner. Res* 2003;18(7):1186–1197. [PubMed: 12854828]
43. Bonewald LF, Harris SE, Rosser J, Dallas MR, Dallas SL, Camacho NP, Boyan B, Boskey A. von Kossa staining alone is not sufficient to confirm that mineralization in vitro represents bone formation. *Calcif. Tissue Int* 2003;72(5):537–547. [PubMed: 12724828]e-publication, 06 May 2003
44. Kato Y, Boskey A, Spevak L, Dallas M, Hori M, Bonewald LF. Establishment of an osteoid preosteocyte-like cell MLO-A5 that spontaneously mineralizes in culture. *J. Bone Miner. Res* 2001;16(9):1622–1633. [PubMed: 11547831]
45. Kuhn LT, Wu Y, Rey C, Gerstenfeld LC, Grynblas MD, Ackerman JL, Kim HM, Glimcher MJ. Structure, composition, and maturation of newly deposited calcium-phosphate crystals in chicken osteoblast cell cultures. *J. Bone Miner. Res* 2000;15(7):1301–1309. [PubMed: 10893678]
46. Clupper DC, Gough JE, Embanga PM, Notingher I, Hench LL, Hall MM. Bioactive evaluation of 45S5 bioactive glass fibres and preliminary study of human osteoblast attachment. *J. Mater. Sci. Mater. Med* 2004;15(7):803–808. [PubMed: 15387416]
47. Silve C, Lopez E, Vidal B, Smith DC, Camprasse S, Camprasse G, Couly G. Nacre initiates biomineralization by human osteoblasts maintained in vitro. *Calcif. Tissue Int* 1992;51(5):363–369. [PubMed: 1458341]
48. Boyan BD, Bonewald LF, Paschalis EP, Lohmann CH, Rosser J, Cochran DL, Dean DD, Schwartz Z, Boskey AL. Osteoblast-mediated mineral deposition in culture is dependent on surface microtopography. *Calcif. Tissue Int* 2002;71(6):519–529. [PubMed: 12232675]
49. About I, Bottero MJ, de Denato P, Camps J, Franquin JC, Mitsiadis TA. Human dentin production in vitro. *Exp. Cell Res* 2000;258(1):33–41. [PubMed: 10912785]
50. About I, Mitsiadis TA. Molecular aspects of tooth pathogenesis and repair: in vivo and in vitro models. *Adv. Dent. Res* 2001;15:59–62. [PubMed: 12640742]
51. About I, Camps J, Mitsiadis TA, Bottero MJ, Butler W, Franquin JC. Influence of resinous monomers on the differentiation in vitro of human pulp cells into odontoblasts. *J. Biomed. Mater. Res* 2002;63(4):418–423. [PubMed: 12115750]
52. Magne D, Bluteau G, Fauchoux C, Palmer G, Vignes-Colombeix C, Pilet P, Rouillon T, Caverzasio J, Weiss P, Daculsi G, Guicheux J. Phosphate is a specific signal for ATDC5 chondrocyte maturation and apoptosis-associated mineralization: possible implication of apoptosis in the regulation of endochondral ossification. *J. Bone Miner. Res* 2003;18(8):1430–1442. [PubMed: 12929932]
53. Boskey AL, Stiner D, Binderman I, Doty SB. Type I collagen influences cartilage calcification: an immunoblocking study in differentiating chick limb-bud mesenchymal cell cultures. *J. Cell Biochem* 2000;79(1):89–102. [PubMed: 10906758]
54. Boskey AL, Doty SB, Stiner D, Binderman I. Viable cells are a requirement for in vitro cartilage calcification. *Calcif. Tissue Int* 1996;58(3):177–185. [PubMed: 8852573]
55. Boskey AL, Camacho NP, Mendelsohn R, Doty SB, Binderman I. FT-IR microscopic mappings of early mineralization in chick limb bud mesenchymal cell cultures. *Calcif. Tissue Int* 1992;51(6):443–448. [PubMed: 1451012]

56. Boskey AL, Paschalis EP, Binderman I, Doty SB. BMP-6 accelerates both chondrogenesis and mineral maturation in differentiating chick limb-bud mesenchymal cell cultures. *J. Cell Biochem* 2002;84(3):509–519. [PubMed: 11813256]
57. Rokita E, Cichocki T, Divoux S, Gonsior B, Hofert M, Jarczyk L, Strzalkowski A. Calcification of the aortic wall in hypercalcemic rabbits. *Exp. Toxicol. Pathol* 1992;44(6):310–316. [PubMed: 1333314]
58. Tomazic BB, Brown WE, Schoen FJ. Physicochemical properties of calcific deposits isolated from porcine bioprosthetic heart valves removed from patients following 2–13 years function. *J. Biomed. Mater. Res* 1994;28(1):35–47. [PubMed: 8126027]Erratum in: *J. Biomed. Mater. Res* 28 (April 1994) (4), 527
59. Tomazic BB. Physiochemical principles of cardiovascular calcification. *Z. Kardiol* 2001;90(Suppl 3):68–80. [PubMed: 11374037]
60. Leyva AG, Maguid SL, Rodriguez de Benyacar MA, Lazaro MA, Cocco JM, Citera G. Pathological mineralizations: calcifications and Si-bearing particles in soft tissues and their eventual relationship to different prostheses. *Artif. Organs* 2000;24(3):179–181. [PubMed: 10759635]
61. Bohic S, Heymann D, Pouezat JA, Gauthier O, Daculsi G. Transmission FT-IR microspectroscopy of mineral phases in calcified tissues. *C. R. Acad. Sci. III* 1998;321(10):865–876. [PubMed: 9835023]
62. Gartner J, Simons B. Analysis of calcific deposits in calcifying tendinitis. *Clin. Orthop* 1990;(254): 111–120. [PubMed: 2157572]
63. McCarty DJ, Lehr JR, Halverson PB. Crystal populations in human synovial fluid. Identification of apatite, octacalcium phosphate, and tricalcium phosphate. *Arthritis Rheum* 1983;26(10):1220–1224. [PubMed: 6626280]
64. Tochon-Danguy HJ, Boivin G, Geoffroy M, Walzer C, Baud CA. Physical and chemical analyses of the mineral substance during the development of two experimental cutaneous calcifications in rats: topical calciphylaxis and topical calcergy. *Z. Naturforsch. [C]* 1983;38(1–2):135–140.
65. Osteoporosis Prevention, Diagnosis, and Therapy. NIH Consensus Statement 2000;17:1–45.
66. Currey JD. The mechanical consequences of variation in the mineral content of bone. *J. Biomech* 1969;2:1–11. [PubMed: 16335107]
67. Oden ZM, Selvitelli DM, Hayes WC, Myers ER. The effect of trabecular structure on DXA-based predictions of bovine bone failure. *Calcif. Tissue Int* 1998;63:67–73. [PubMed: 9632849]
68. Currey JD. The many adaptations of bone. *J. Biomech* 2003;36:1487–1495. [PubMed: 14499297]
69. Currey JD, Brear K, Zioupos P. The effects of aging and changes in mineral content in degrading the toughness of human femora. *J. Biomech* 1996;21:257–260. [PubMed: 8849821]
70. Boskey AL. Bone mineral and matrix. Are they altered in osteoporosis? *Orthop. Clin. N. Am* 1990;21:19–29.
71. Paschalis EP, Betts F, DiCarlo E, Mendelsohn R, Boskey AL. FTIR microspectroscopic analysis of human iliac crest biopsies from untreated osteoporotic bone. *Calcif. Tissue Int* 1997;61:487–492. [PubMed: 9383276]
72. Mendelsohn, R.; Camacho, NP.; Boskey, AL. AL. Infrared Microscopy and Imaging of Hard and Soft Tissues: Applications to Bone, Skin, and Cartilage. In: Levin, I., editor. *Biospectroscopy*. Blackwell Press; in press
73. Camacho NP, Landis WJ, Boskey AL. Mineral changes in a mouse model of osteogenesis imperfecta detected by Fourier transform infrared microscopy. *Connect. Tissue Res* 1996;35(14):259–265. [PubMed: 9084664]
74. Camacho NP, Hou L, Toledano TR, Ilg WA, Brayton CF, Raggio CL, Root L, Boskey AL. The material basis for reduced mechanical properties in oim mice bones. *J. Bone Miner. Res* 1999;14(2): 264–272. [PubMed: 9933481]
75. Sims TJ, Miles CA, Bailey AJ, Camacho NP. Properties of collagen in OIM mouse tissues. *Connect. Tissue Res* 2003;44(Suppl 1):202–205. [PubMed: 12952198]
76. Boskey A. Mineral changes in osteopetrosis. *Crit. Rev. Eukaryot. Gene Exp* 2003;13(2–4):109–116.
77. Faibish D, Gomez A, Boivin G, Binderman I, Boskey A. Infrared imaging of calcified tissue of bone biopsies from adult osteomalacia. *Bone*. in press

78. Grant GA, Wener MH, Yaziji H, Futran N, Bronner MP, Mandel N, Mayberg MR. Destructive tophaceous calcium hydroxyapatite tumor of the infratemporal fossa. Case report and review of the literature. *J. Neurosurg* 1999;90(1):148–152. [PubMed: 10413170]
79. Camacho NP, Carroll P, Raggio CL. Fourier transform infrared imaging spectroscopy (FT-IRIS) of mineralization in bisphosphonate-treated oim/oim mice. *Calcif. Tissue Int* 2003;72(5):604–609. [PubMed: 12574874]e-publication, 10 February 2003
80. Paschalis EP, Burr DB, Mendelsohn R, Hock JM, Boskey AL. Bone mineral and collagen quality in humeri of ovariectomized cynomolgus monkeys given rhPTH(1–34) for 18 months. *J. Bone Miner. Res* 2003;18:769–775. [PubMed: 12674338]
81. Otomo H, Sakai A, Ikeda S, Tanaka S, Ito M, Phipps RJ, Nakamura T. Regulation of mineral-to-matrix ratio of lumbar trabecular bone in ovariectomized rats treated with risedronate in combination with or without Vitamin K2. *J. Bone Miner. Metab* 2004;22(5):404–414. [PubMed: 15316861]
82. Faibish D, Ott S, Boskey A. Mineral changes in osteoporosis. *Clin. Orthop.* in review
83. Paschalis EP, Boskey AL, Kassem M, Eriksen EF. Effect of hormone replacement therapy on bone quality in early postmenopausal women. *J. Bone Miner. Res* 2003;18:955–959. [PubMed: 12817747]
84. Boskey, AL.; Karsenty, G.; McKee, MD. Mineral characterization of bones and soft tissues in matrix gla protein deficient mice. In: Goldberg, M.; Boskey, A.; Robinson, C., editors. *Chemistry, Biology of Mineralized Tissues*. American Academic Orthopaedic Surgeons; Chicago, IL: 2000. p. 63–67.
85. Atti E, Boskey AL, Canalis E. Overexpression of IGF-binding protein 5 alters mineral and matrix properties in mouse femora: an infrared imaging study. *Calcif. Tissues*. 2004e-publication, 18 November

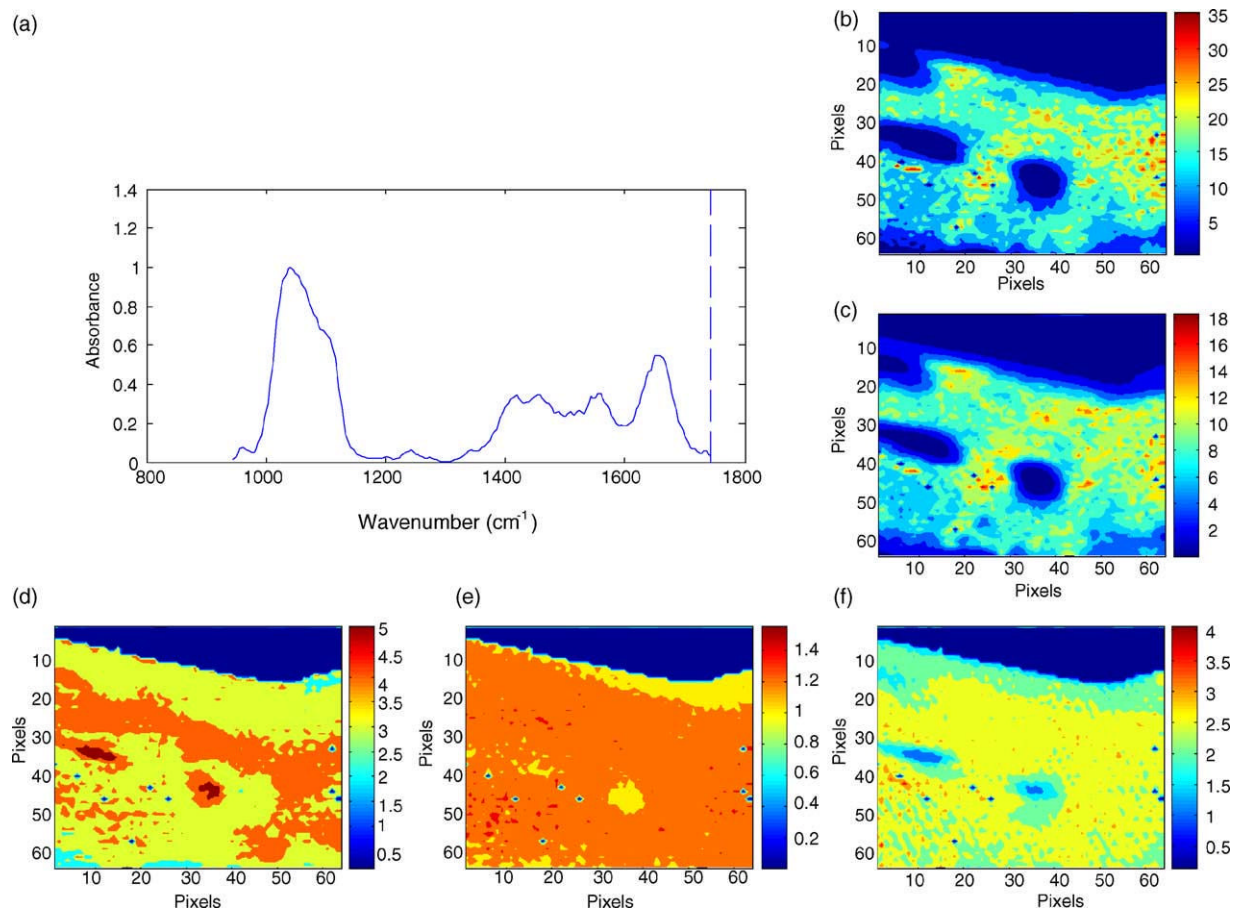


Fig. 1.

Hyperspectral images of bone mineral properties: in normal human cortical bone (a) typical spectrum from a single image pixel, (b) image of the mineral distribution in the biopsy, (c) image of the matrix distribution in the biopsy, (d) image of carbonate distribution, (e) image of mineral:matrix ratio, (f) image of crystallinity and (g) image of collagen cross link ratio.

Note: all images are corrected for the presence of the embedding media, PMMA.

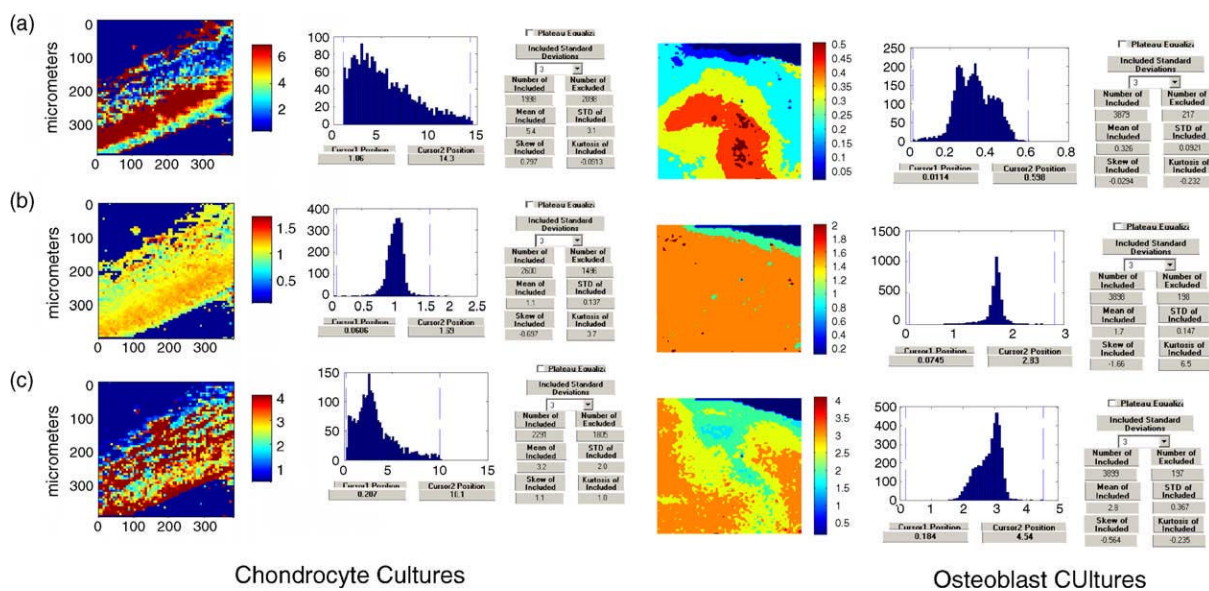


Fig. 2. Images of mineralizing chondrocyte (left) and osteoblast (right) cultures: (a) mineral:matrix ratio, (b) crystallinity and (c) collagen cross-link ratio.

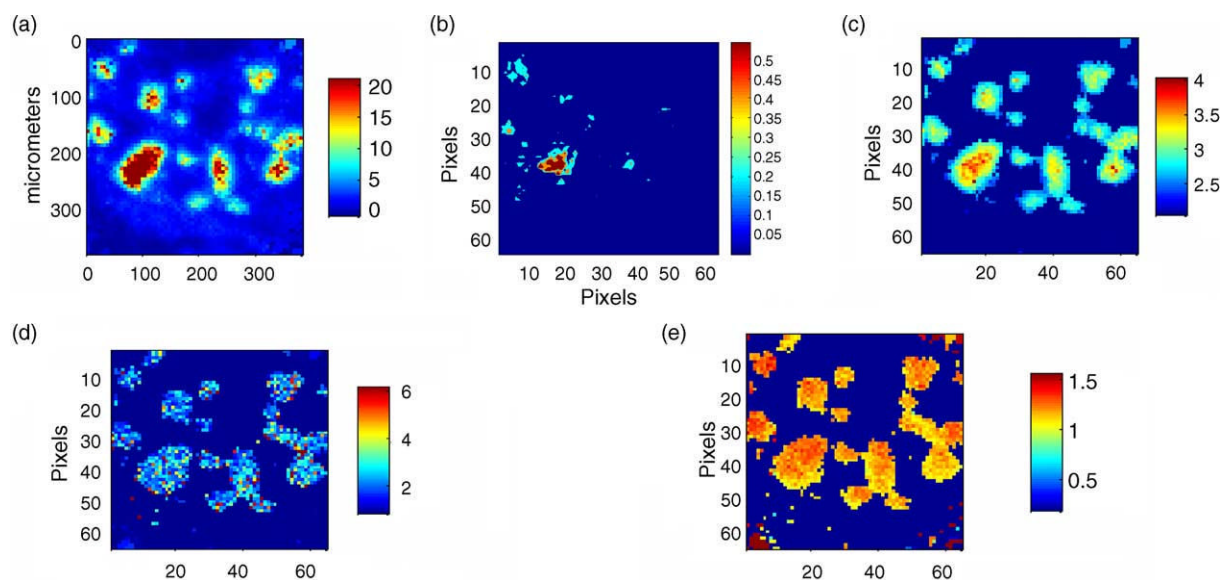
**Fig. 3.**

Image of a pathologic deposit removed from a patient with juvenile dermatomyositis: (a) mineral distribution, (b) lipid distribution, (c) mineral:matrix ratio (d) collagen cross-link ratio and (e) crystallinity distribution.

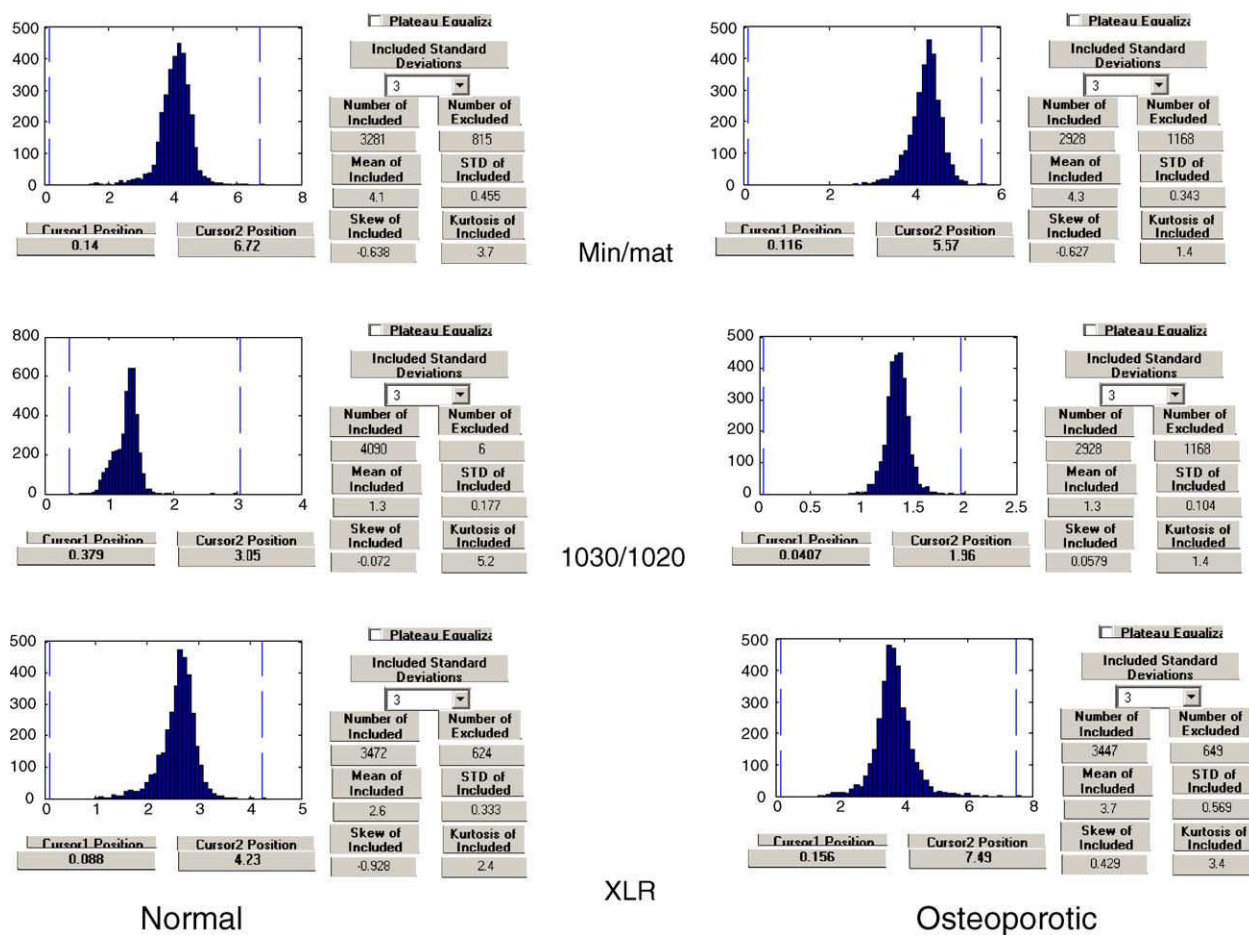


Fig. 4.
Pixel histograms for the average distribution of mineral:matrix, crystallinity and collagen cross link ratio in normal and osteoporotic biopsies.

Table 1

Vertebrate calcified tissues

Physiologic			Dystrophic		
Tissue	Mineral	Matrix	Tissue/disease	Mineral	Notes
Bone	Hydroxyapatite	Collagen	Atherosclerotic plaques	Hydroxyapatite	Lipid involvement
Calcified cartilage	Hydroxyapatite	Collagen	Prosthetic heart valves	Hydroxyapatite	Collagen based
Tendon and ligament insertions	Hydroxyapatite	Collagen	Tumoral calcinosis	Hydroxyapatite	Juxta-articular space
Cementum	Hydroxyapatite	Collagen	Juvenile dermatomyositis	Hydroxyapatite	Muscle and fat deposits
Dentin	Hydroxyapatite	Collagen	Milk alkali disease	Hydroxyapatite	Vitamin D toxicity
Enamel	Hydroxyapatite	Amelogenin enamelin	Kidney stones and salivary stones	Calcium oxalate, whitlockite, hydroxyapatite	
			Thalassemia	Iron oxides	Skin deposits related to transfusions
			Articular cartilage and intervertebral disk deposits	Calcium pyrophosphate dihydrate, monosodium urate, hydroxyapatite, calcium oxalate	

Table 2

Knockout and transgenic mice evaluated by vibrational spectroscopy reveal significant variations from wildtype animals

Protein	Genetic modification	Technique used	Observed changes relative to age and background matched wildtype	Ref.
Type X collagen	Minigene insertion	FTIR-MS	Disordered mineral distribution	[30]
Type X collagen	Knockout	FTIR-MS	Disordered mineral distribution, no change in crystallinity	[32]
Osteocalcin	Knockout	FTIR-MS	Increased mineral content with no change in crystallinity (older animals only)	[34]
Matrix gla protein	Knockout	FTIR-MS, FTIRI	Increased mineral content, increased crystallinity	[84]
Biglycan	Knockout	FTIR-MS	Decreased mineral content, increased crystal size	[33]
Type I collagen	Natural mutation	FTIR-MS	Decreased mineral content, increased acid phosphate content	[73, 79]
Type I collagen	Knockin/transgenic	Raman	Age dependent changes in mineral content but not crystallinity account for mechanical adaptation	[38]
Osteopontin	Knockout	FTIR-MS	Increased mineral content, increased crystallinity	[35]
Osteonectin	Knockout	FTIR-MS, FTIRI	Higher mineral content, greater crystallinity, increased collagen cross links	[36]
Dentin matrix protein 1	Knockout	FTIRI	Decreased bone mineral content, increased crystallinity and collagen cross-link ratio	U
TGF-beta	Knockout	FTIRI	Decreased crystallinity, collagen cross-link ratio, nd mineral content in cortical bone and secondary ossification center	[29]
IGF 1-binding protein	Transgenic	FTIRI	Decreased bone mineral content and collagen cross-link ratio without change in crystallinity	[85]
Dentin sialo-phosphoprotein	Knockout	FTIRI	Decreased bone mineral content, increased crystallinity and collagen cross-link ratio	U
Vitamin D receptor	Transgenic	FTIR-MS	Decreased mineral content, no change in other parameters	[37]
Tissue specific alkaline phosphatase	Knockout	FTIR-MS	Decreased mineral content	[39]

FTIR-MS: FTIR micro-spectroscopy; FTIRI: FTIR imaging; U: unpublished.